Chapter

Application of Seismic Tomography and Geotechnical Modeling for the Solution of Two Complex Instability Cases

Roberto Balia and Pier Paolo Manca

Abstract

The geotechnical instability of sites and artificial structures is a widespread problem that particularly affects heavily anthropized areas and historical cities, and often this instability is linked to human activities and to interventions carried out without adequate preliminary geotechnical studies. The most common procedure for assessing unstable sites includes base studies such as drilling boreholes, shallow excavations, and engineering geology studies. However, more and more often, some geophysical techniques are associated to the above intervention, represent the first phase of assessment, and allow optimizing the possible campaign of excavations and boreholes. Compared to direct surveys, the geophysical ones provide extensive and continuous information, are moderately invasive, and have a remarkably advantageous information-to-cost ratio. In this chapter, we illustrate two examples of characterization of unstable sites. The first case concerns the ancient walls of an Italian city, and the second one deals with the instability of a road slope. In both cases, the geotechnical modeling is also based on the results of preliminary geophysical surveys.

Keywords: slope instability, structure instability, geotechnical modeling, geophysical methods, refraction tomography

1. Introduction

Very often, the instability of sites and artificial structures is attributable to human activities and to interventions carried out without special preliminary geotechnical studies. The most common procedure for assessing unstable sites includes base studies such as drilling boreholes, shallow excavations, and engineering geology studies. More and more often, some geophysical surveys are associated to the above intervention, represent the first phase of assessment, and allow optimizing the possible campaign of excavations and boreholes. The geophysical methods provide extensive and continuous information (usually along sections not necessarily vertical), are moderately invasive, and are convenient from an economic point of view. Two assessment examples of unstable sites are illustrated here. The first case concerns the ancient walls of an Italian city, and the second case concerns a slope on which develops a road.

2. Geotechnical modeling

The combined use of geophysical surveys and geomechanical modeling can make it possible to solve complex geotechnical problems for which geognostic surveys alone prove insufficient [1]. As illustrated graphically in **Figure 1**, the proposed procedure is composed of different phases. These are (1) analysis, (2) measurements, (3) processing, (4) preliminary model, (5) in situ surveys, (6) model revision, and (7) back and sensitivity analysis [2]. The above phases are connected to each other in an iterative way as indicated in the graph, until a satisfactory level of coherence between processing results and direct observations is reached. Actually, there may be cases in which it is difficult to know with precision the complete geometry of the problem, the lithology, and the mechanical properties of natural or artificial materials, as they are not directly investigated. In the present cases, it is possible to carry out iterative evaluations in which the formulation of an initial geomechanical model suggests typology and modality of in situ investigations. In other terms, the initial model integrates and improves the interpretative capacity of the geomechanical model whose processing, in turn, must be compared with direct observations (back analysis or inverse problem). The latter observations could be the observed stability or the instability witnessed, for instance, by easily detectable break surfaces. The last phase of the procedure consists of the sensitivity analysis [3].

Thus, we arrive at the calculation of a safety factor in instability or dimensioning of a stabilization intervention or dimensioning of an additional work that modifies the initial situation without altering the original equilibrium or designing a future monitor system. The two real cases are discussed below.

The first one deals with an excavation in the historic city center for the construction of an underground car parking, in an area flanking a sixteenth century bastion of unknown construction features; the second case is a highway slope affected by rotational instability [4].

In both cases, it is necessary to have a definitive geomechanical model, based on which to design interventions whose effects must be foreseen, starting from initial uncertainties on geometrical and geomechanical aspects. In both cases, the procedure develops starting from direct observations and special in situ investigations. The latter allows to apply a back analysis procedure (or inverse solution) able to highlight critical aspects of the problem and/or to refine the forecast geomechanical model.

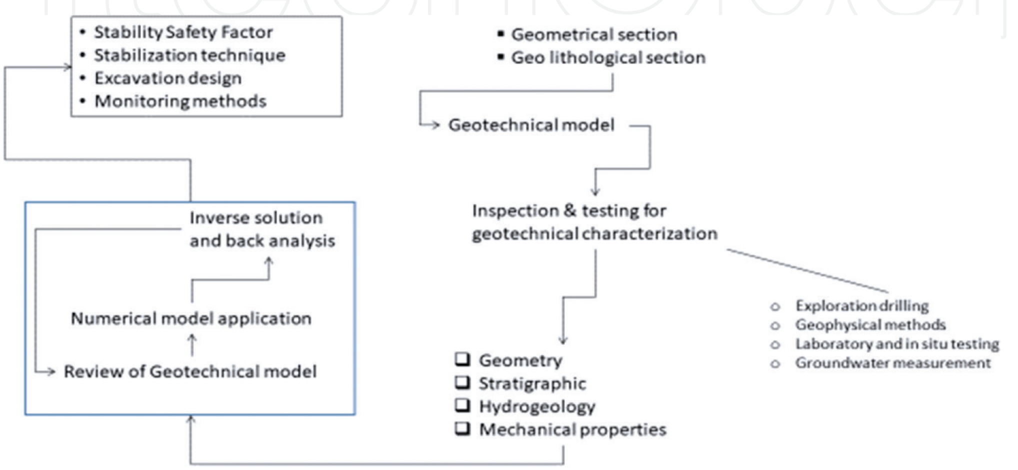

Figure 1.
Flowchart of an iterative analysis modeling—inverse solution.

In the case of the excavation for the construction of the underground car parking, the uncertainties relate to the geometry, composition, and geomechanical properties of the adjacent bastion, obviously apart from the direct observation of the current equilibrium conditions.

In the case of the landslide road, the uncertainties regard the composition of the slope, the stratigraphy and geomechanical properties, and the interaction with a temporary groundwater activated by extraordinary meteoric contributions [5], apart from the direct observation of the landslide in progress.

In both cases, the in situ investigations cannot be exhaustive, due to the discontinuity of the acquired information and to uncertainties implicit in the methodology followed.

Although the nature of the two problems is not the same—feared instability in one case and already occurred instability in the other—they lend themselves to exemplifying the possibility of identifying solutions through the combined action between the geomechanical model and in situ surveys. Among the latter, geophysical-geognostic surveys are those that offer the possibility to acquire the most information possible, by extension and quality.

3. Geophysical investigations

3.1 Geophysical techniques and geotechnical model: the seismic tomography

The most common procedures for recognizing unstable sites include drilling boreholes, shallow excavations, and engineering geology studies. However, more and more often, some geophysical techniques are associated to the above intervention, and usually they represent the first phase of assessment and allow optimizing the campaign of excavations and boreholes. Compared to direct surveys, the geophysical ones provide extensive and continuous information (usually along sections not necessarily vertical), are moderately invasive and have a remarkably advantageous information-to-cost ratio.

Among the various geophysical methods, the seismic ones (e.g., [6]) are the most widely used for geotechnical purposes. The reason is that the velocity of propagation of the elastic (or seismic) waves depends on the density and the elastic properties of the medium in which they propagate. The seismic methods are of different types: first of all the classical seismic refraction, seismic reflection, and the seismic tomography methods. In recent decades, some more methods based on the analysis of the surface wave's dispersion, such as the MASW, multichannel analysis of surface waves; the SASW, spectral analysis of surface waves; and the REMI, refraction microtremor, have been added [7].

Geophysical prospecting methods based on the refraction of seismic waves date back to the 1920s of the last century, mainly in the field of petroleum research. Over time, refraction techniques for oil and gas research have been progressively supplanted by reflection techniques, and their use has shifted to other prospecting fields with objectives falling within the first hundred meters of depth. Actually, the classical seismic refraction shooting based on the analysis and interpretation of the travel time curves has been widely used in the geotechnical field, especially in the study of foundation soils and slope stability. However, before the 1980s of the last century, the processing of seismic refraction data provided approximate models, except in cases of quite regularly layered subsoil. An important step was made with new processing techniques, first the GRM, generalized reciprocal method [8], but still the work was done in terms of seismic rays substantially conceived and represented as broken lines, and only the main refractors could be highlighted. With respect to geotechnical study field, the most important leap, leading to current refraction data processing, has been the operational advent of the seismic tomography [9]. Among the numerous scientific works concerning the topic, the one of White [10] is undoubtedly worth mentioning. As for the inversion algorithm, the most used were FBP, filtered back projection; ART, algebraic reconstruction technique; and SIRT, simultaneous iterations reconstruction technique. In the examples discussed here, the inversion algorithm named ASA—adaptive simulated annealing [11]—has been used. In the seismic tomography, data acquisition is carried out with ordinary energy sources, such as hammers, dropping masses, downhole energy sources, and small charges of dynamite, and with standard receivers such as electromagnetic geophones and piezoelectric hydrophones. **Figures 2**–**4** show the most common acquisition schemes in seismic tomography. The first one is the classical refraction tomography with both shots and receivers at the ground surface; the second, in **Figure 3**, is the cross-hole tomography where both shots and receivers are placed inside boreholes, better if filled with water; the third, in **Figure 4**, is the up-hole tomography. Referring to **Figure 4**, if the position of shots and detectors is inverted (i.e., the detectors are placed inside the borehole and the shots are placed at the ground surface), the acquisition system is properly named "downhole tomography." It must be underlined that though in the schematic sketch of both cross-hole and up-hole, the ray paths are rectilinear, and this can

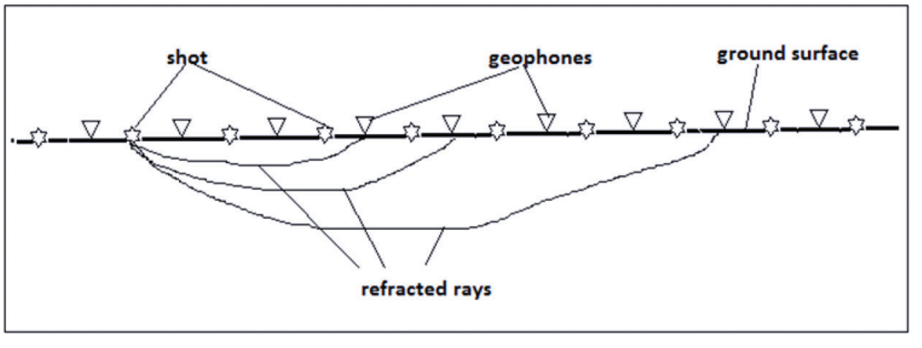

Figure 2.
Acquisition system of the classical seismic refraction tomography.

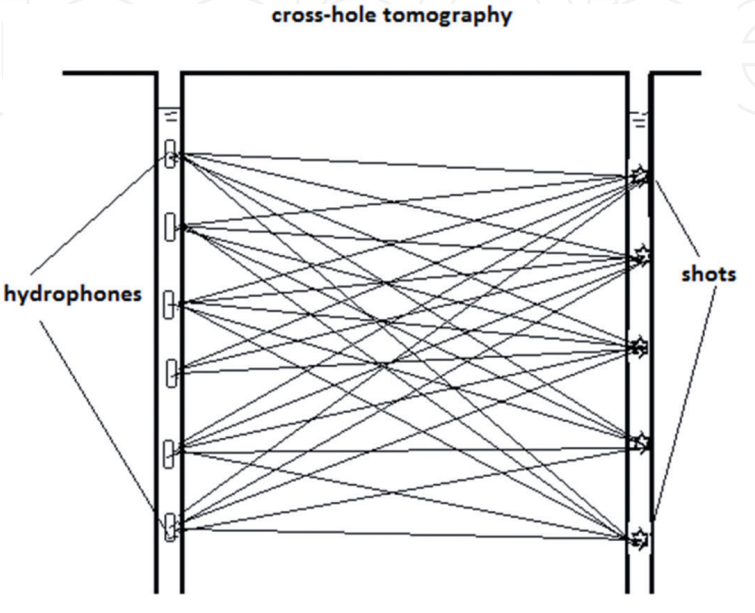

Figure 3.
Acquisition system of the seismic up-hole tomography.

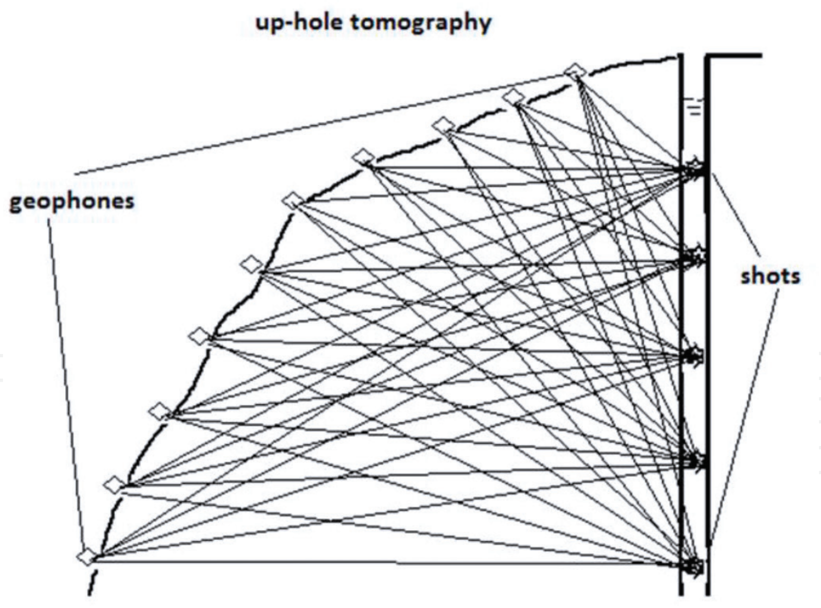

Figure 4.
Acquisition system of the seismic cross-hole tomography.

happen only when the subsoil is homogeneous and isotropic, otherwise, ray paths are curvilinear due to refraction.

3.2 First case study: the ancient walls of the city of Cagliari (Sardinia, Italy)

The study area lies in the northwestern sector of the ancient walls of Cagliari. Apart from the Roman works, of which few traces remain, the original body of the walls, built by the Pisans (Republic of Pisa), dates back to the thirteenth century; in literature, these walls are also referred to as "the Pisan walls" or "the medieval walls." Three centuries later—that is, in in the sixteenth century, after the advent of firearms, in particular the artillery—the Spanish, who at that time dominated Cagliari, decided to modify the defense line incorporating the medieval walls in an embankment coated with limestone blocks; the latter, apart from few modifications and consolidation works, is the current structure of the walls. **Figure 5** shows in detail (the circle) the area in which two up-hole tomographies have been carried out

Figure 5.
The northwestern sector of the Spanish walls. The circle indicates the survey area.

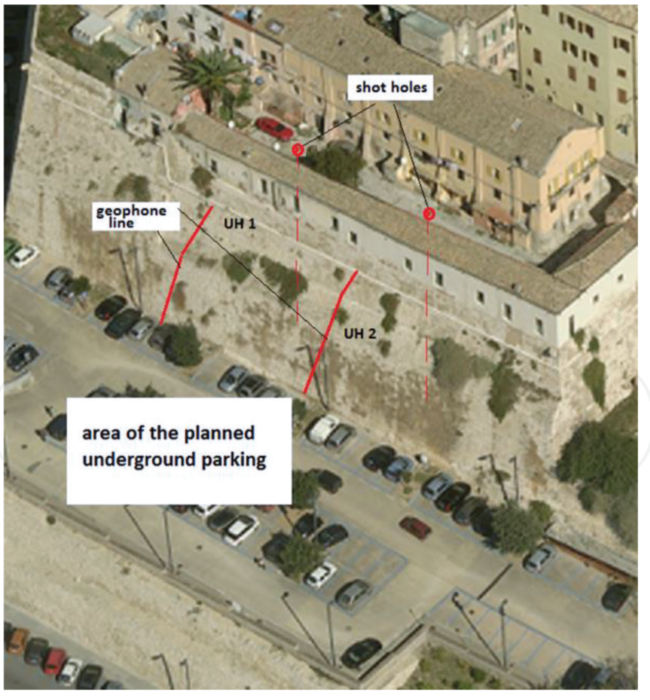

Figure 6.
Position of the two acquisition arrays.

to provide information for the geotechnical modeling of the walls, in view of the construction of an underground car parking, right at the foot of the walls itself.

As for data acquisition geometry, the geophones were placed on the outer surface of the coating at intervals of 1.6 m, and the shots were performed in their respective holes at 1–2 m spacing, starting from the bottom.

Data processing has been performed by means of a software based on a nonlinear optimization technique (ASA, adaptive simulated annealing) [11] that works in terms of modeling, starting from the set of the first arrival times and the spread geometry. **Figure 6** shows the position of the two acquisition arrays, and **Figure 7** shows their schematic view. The results after processing and interpretation are in

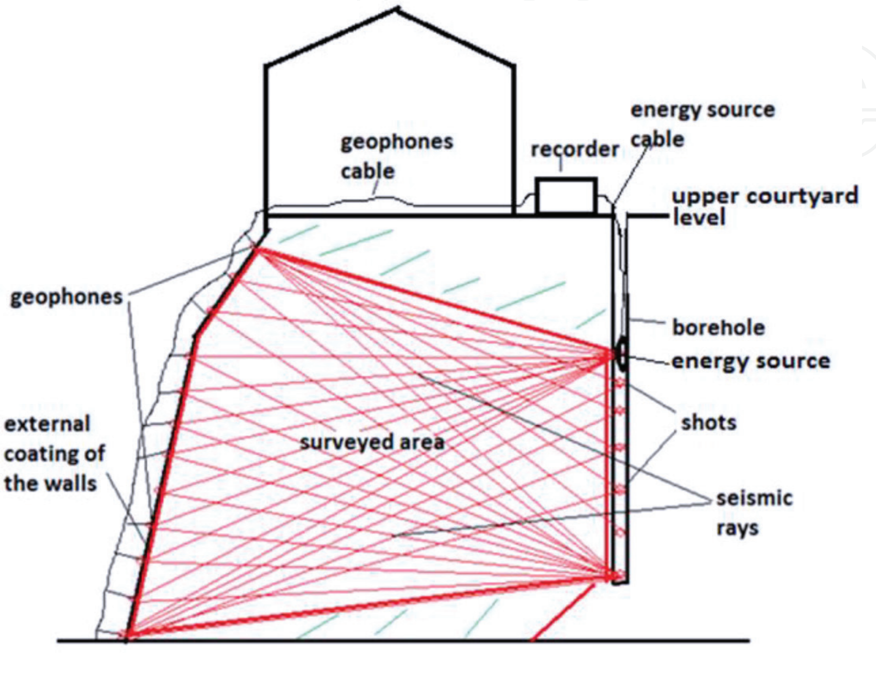

Figure 7.
Schematic view of the up-hole seismic tomographies across the ancient walls.

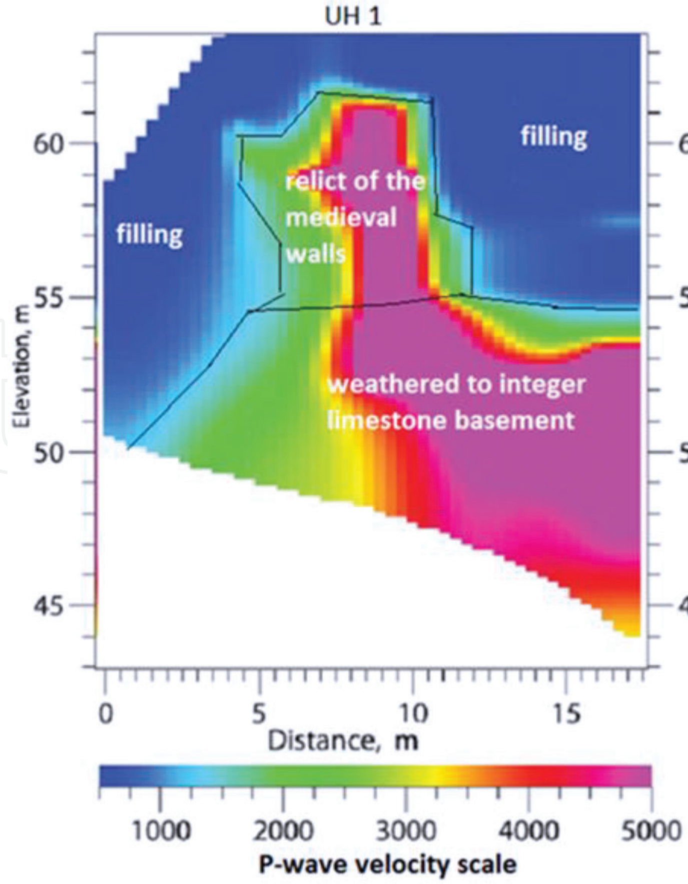

Figure 8.
Up-hole tomography UH1 interpreted.

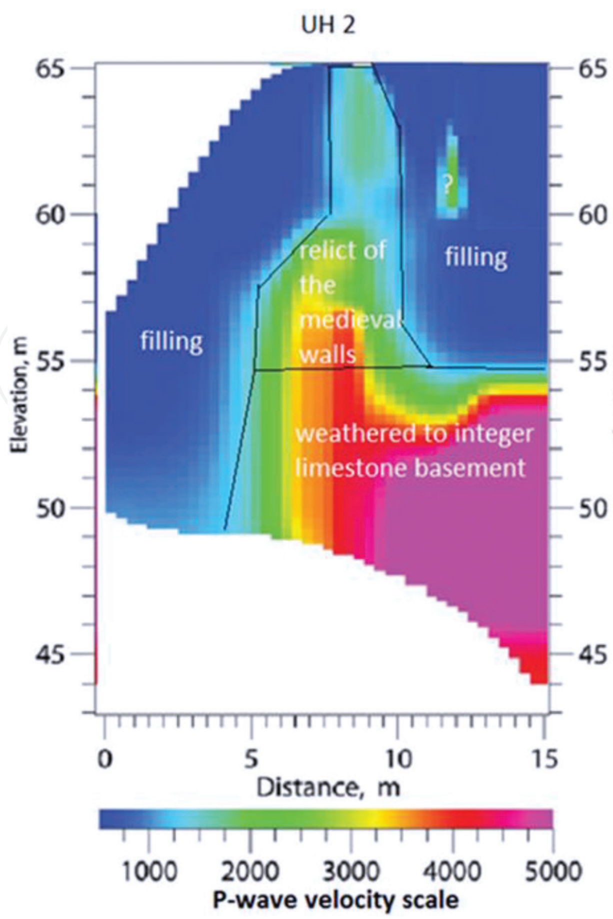

Figure 9.
Up-hole tomography UH2 interpreted.

Figures 8 and **9**. The two tomographies show very similar characteristics, and the ancient medieval wall, the limestone basement, and the filling on both sides of the medieval wall are clearly depicted. On the contrary, the tomographies show no trace of the external coating of the current walls, though its presence is certain. This is a clear sign that thickness of the coating is relatively small and therefore has not been covered satisfactorily by the seismic rays, as deductible from **Figure 7**.

From the two up-hole tomographies and several drillings, the base model for the geotechnical assessment has been compiled as shown in **Figure 10**.

3.3 Second case study: a road embankment along a hillside

Figure 11 shows a satellite view of a road that runs along the side of a hill in Sardinia, Italy. A few years from the construction of the road, after an exceptionally rainy season, progressively pronounced fracture lines, indicated in the figure, appeared on the asphalt. It was the beginning of a landslide that affected the background and the road itself. **Figure 12** shows a detail of a fracture. After 1 month of monitoring, since fracturing—and therefore the landslide—progressed, it was decided to verify the conditions of the subsoil through geophysical techniques. Then, two seismic refraction tomographies perpendicular to the axis of the road, as shown in **Figure 13**, were executed. Data acquisition was carried out with a 48-geophone spread, detector interval of 2.7 m, and same interval for shots (hand hammer with vertical stacking); the processing was performed with the same software employed in the previous case study. The position of the two seismic lines is in **Figure 13**, and the two P-wave velocity sections are in **Figures 14** and **15**.

Tomography SRT1 (**Figure 14**) exhibits a surface zone 5–14 m thick that extends along the whole section. It is composed of the natural unconsolidated overburden and the artificial body of the road embankment, with P-wave velocity in the range 400–800 m/s. The underlying marls are initially much altered for a thickness in the range 2–10 m. Worth of notice is that just under the road, there is a 15–20 m wide zone that deepens for about 20 m, in which, after the demolition of the embankment, water was found. At the base, at depths of 15–20 m from the surface, except

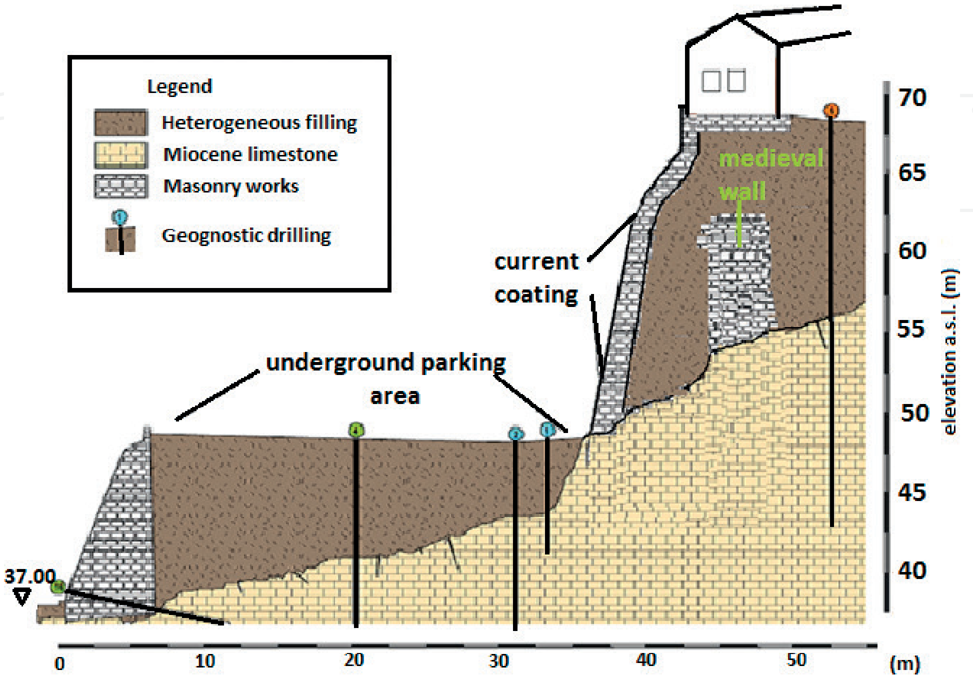

Figure 10.
Geotechnical model deduced from the two up-hole seismic tomographies and four geognostic boreholes indicated in the figure.

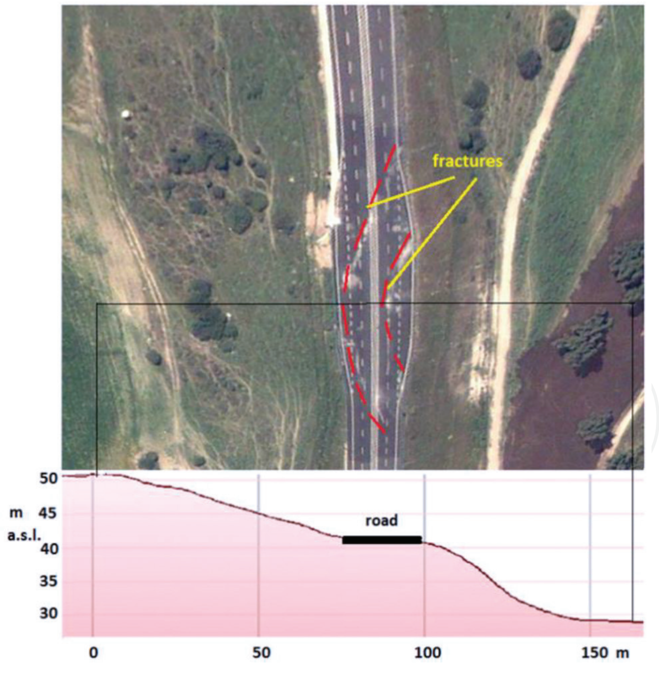

Figure 11.
The stretch of road affected by the landslide phenomenon and the elevation profile.

Figure 12.
Detail of a fracture in the asphalt at the beginning of the landslide phenomena.

Figure 13.
Position of the two seismic refraction tomographies.

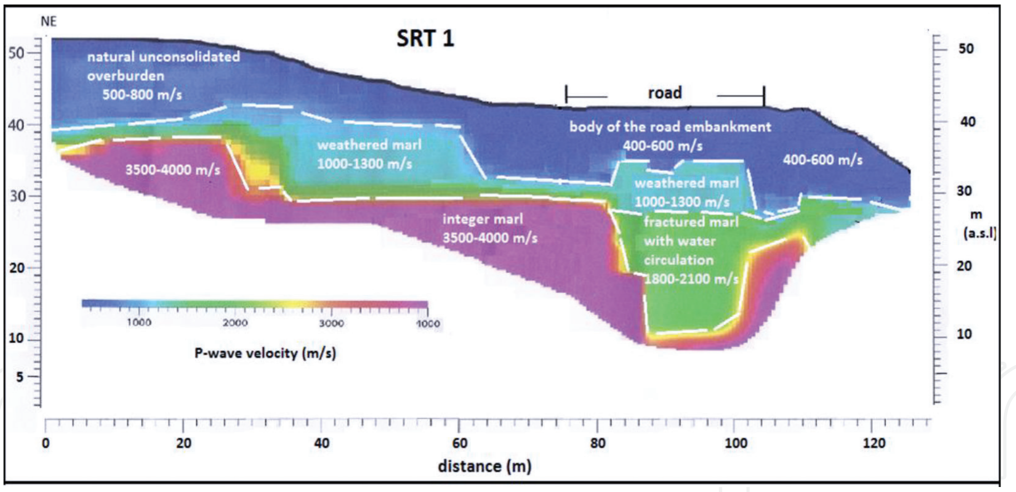

Figure 14.
Seismic refraction tomography SRT 1 interpreted.

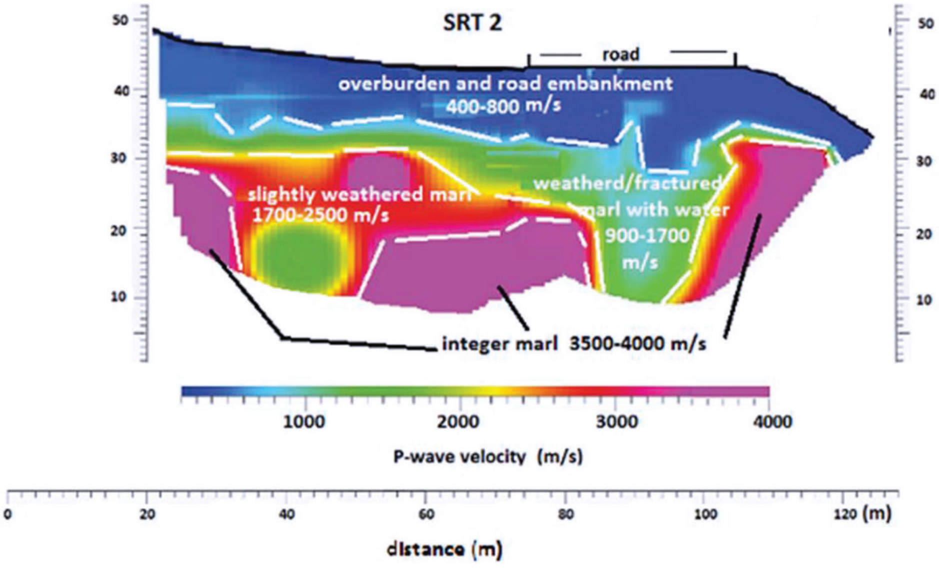

Figure 15.
Seismic refraction tomography SRT 2 interpreted. The SRT 2 is parallel to SRT 1, and the scale indicates the alignment.

in the abovementioned area below the road, there are integer marls. At least three faults can be identified.

The seismic tomography SRT 2 (**Figure 15**) exhibits features similar to those of SRT 1. In this case at least two faults can be identified. The two tomographies will constitute the basis for the road slope stability study.

4. Stability analysis of Spanish walls

4.1 Identification of the geotechnical problem

The geotechnical problem consists of the need of predicting the effects of the excavation in the area adjacent to the bastion and to assess the risk of compromising the stability of the latter. The geognostic and geophysical investigations made it possible to define the internal composition of the bastion and the physical properties of the materials, but they do not allow identifying the actual dimensions of the external coating, that is, the containment wall, and leave uncertain the mechanical properties of the materials, such as the cohesion and the internal friction angle of the Mohr Coulomb model. However, the geognostic and geophysical surveys have made it possible to reconstruct a geomechanical model, whose completion requires a sensitivity analysis of

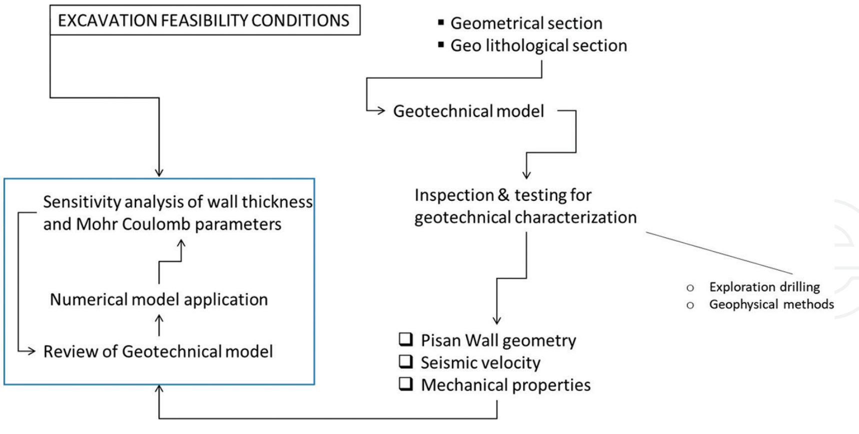

Figure 16.
Case 1: flowchart of iterative analysis modeling—inverse solution.

the results as the geometric and geomechanical characteristics of the external containment wall of the bastion vary. **Figure 16** shows the flowchart of the whole procedure.

4.2 Modeling and results

Calculations were set based on reliable values of geotechnical properties (**Table 1**) called "hypothesis B" and four values (2.5, 2.0, 1.5, and 1.0 m) of the wall thickness. The modeling process allows the calculation of the safety factor (SF) in the three

Material	γ kg m^{-3}	ϕ °	C kPa	σ_tkPa
Rock basement	2500	35	350	130
Spanish coating	2500	35	350	130
Pisan walls	2500	35	350	130
Filling material	1600	35	10	0
Overload	50	—	—	—

Table 1.
Geotechnical properties of the materials for the hypothesis B.

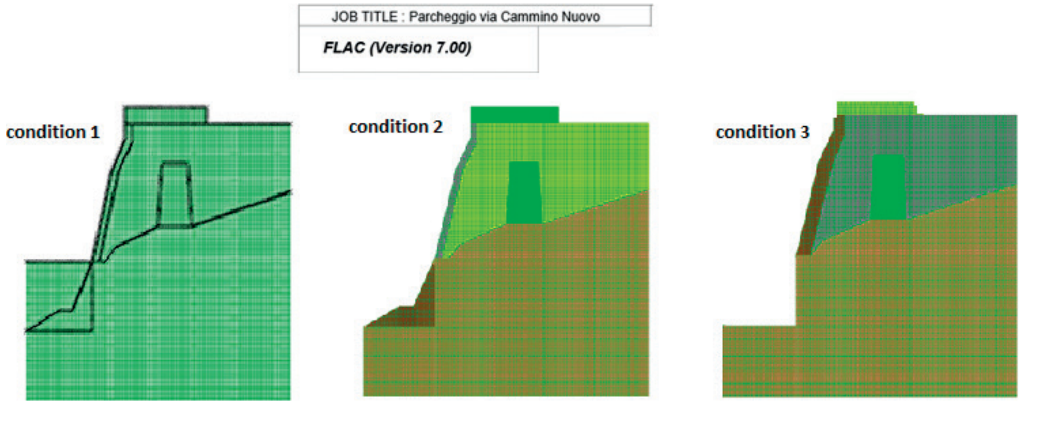

Figure 17.
Left to right: pre-excavation, first excavation, and second excavation.

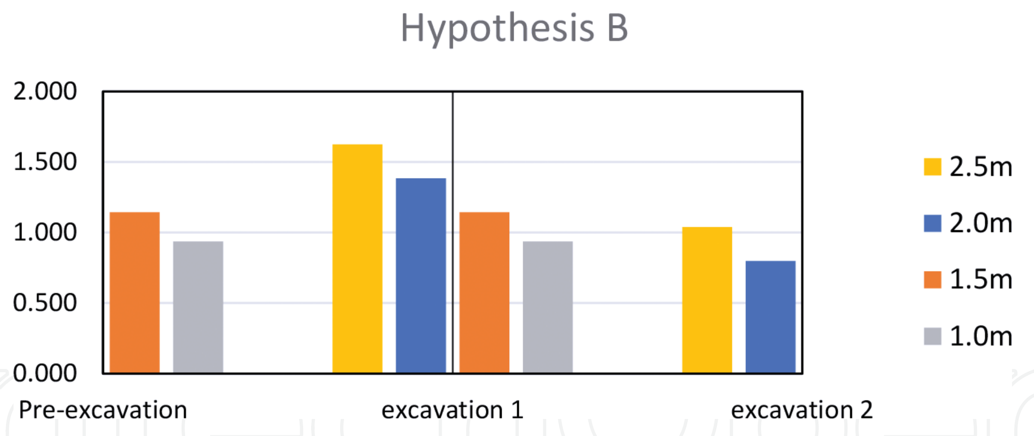

Figure 18.
Results for the hypothesis B: SF versus excavation steps and wall thickness (m).

possible excavation steps, that is, (1) without excavation, (2) excavation of the only loose material, and (3) excavation extended to a portion of the underlying rock (**Figure 17**). The results are shown in histograms of **Figure 18**.

The hypothesis B has been modified in A and C that differ for the cohesion and the tensile strength. The results obtained are illustrated in the diagrams of **Figure 19**.

4.3 Feasibility of excavation

The results obtained show that:

- Changes in the mechanical properties result in unimportant changes in the SF. For variations of cohesion in a range of ±20% and of the tensile strength of ±40%, the corresponding SF values vary by only ±5%.

- The realization of the first excavation, that is, the removal of the ground in front of the wall (**Figure 17**), does not cause significant SF variations that can

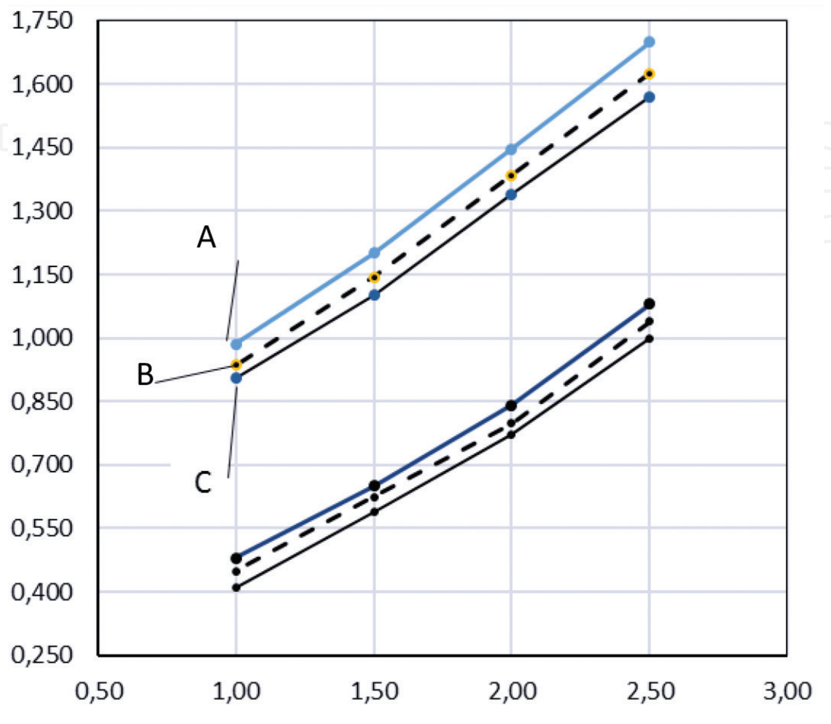

Figure 19.
SF versus wall thickness (m) for A, B, and C hypotheses of mechanical properties.

be considered constant (see **Figure 18**) for any wall thickness. The subsequent excavation n.2, corresponding to the removal of a rock portion, determines reductions in the SF (see diagrams in **Figures 18** and **19**) between 30% and 55%. As less thick is the wall as smaller is the SF (see **Figure 20**).

- The possibility and the ways of carrying out the excavation in front of the wall are linked to the verification of its thickness.

In summary, in all the cases examined, the execution of the excavation must always be preceded by retaining structures; these must concern only the base of the wall, if only the first excavation will be carried out, or even the rock wall, if the second excavation will be carried out. The retaining structures design will have to consider the effective thickness of the wall and will have most important and binding extension, the lower the measured thickness will be (**Figure 20**).

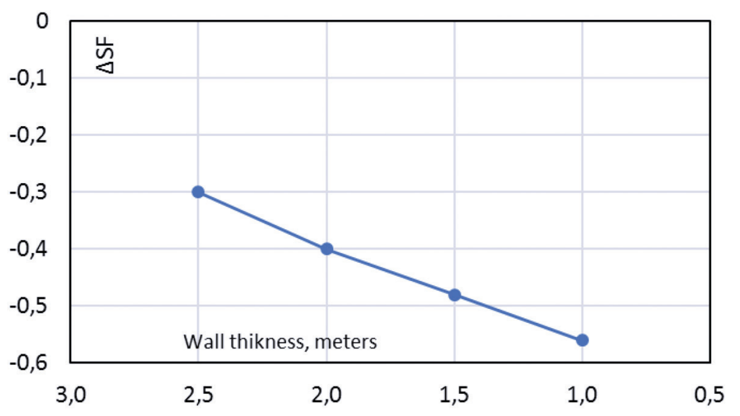

Figure 20.
SF reduction for the second excavation versus wall thickness (meters).

5. Road slope stability

5.1 Identification of the geotechnical problem and modeling results

In the second case, the geotechnical problem is represented by a slope instability, apparently unjustified even in the case of poor geotechnical properties of the materials but occasionally worsened by groundwater from a nearby stream [12, 13].

Rock type	Density, kg m^{-3}	Young's modulus, MPa	Poisson's ratio	Cohesion, kPa	Friction angle	Tensile strength, kPa
Compact marl	2300	500	0.25	200	35°	50
Altered marl	2100	250	0.25	0–5 to 10–15	30°	0
Arenaceous rock	2000	100	0.30	10–15	30°	0
Fill road material	1600	50	0.30	10–15	25°	0

Table 2.
Geotechnical properties of the materials.

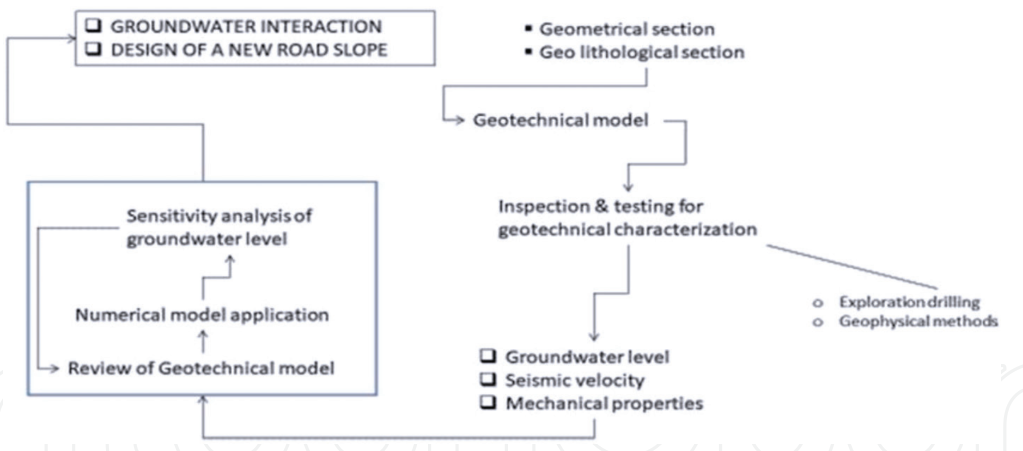

Figure 21.
Case 2: flowchart of iterative analysis modeling—Sensitivity calculations.

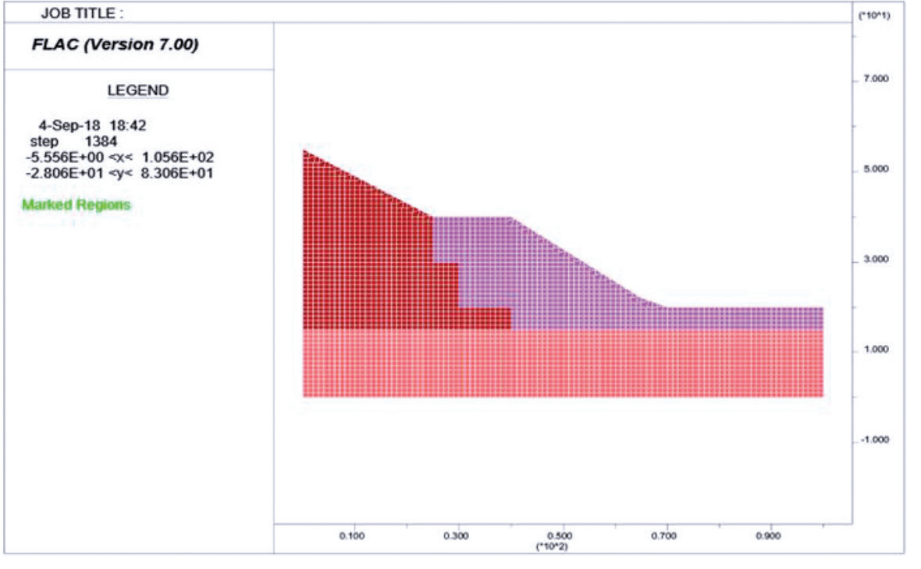

Figure 22.
Numerical model of the slope.

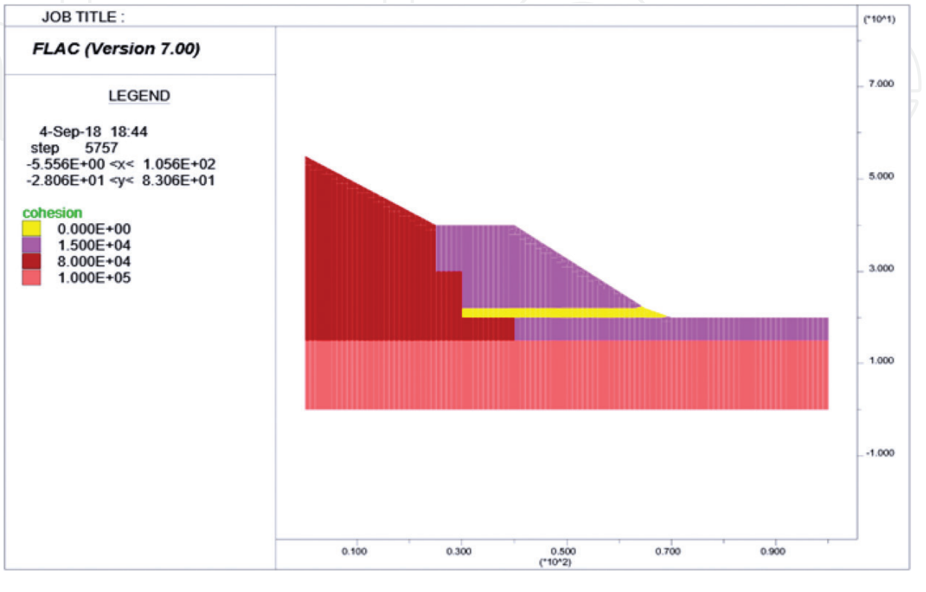

Figure 23.
Cohesion of the different materials.

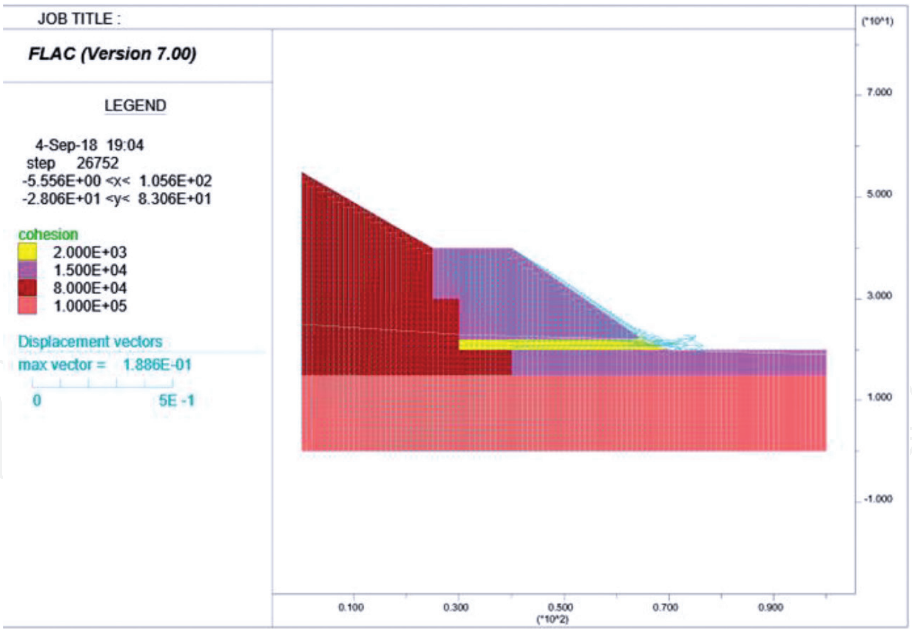

Figure 24.
Displacement vectors of the slope instability.

In accordance with the results of exploration drilling and geophysical survey (see geotechnical properties in **Table 2** and flowchart of **Figure 21**), a geotechnical model was reconstructed whose solution was obtained with numerical methods and the application of the 2D FLAC software [2] (see **Figures 22–24**).

The numerical model was corrected according to an iterative procedure to reconstruct the instability mechanism observed in situ. The next step was to highlight the effects of a growing groundwater. The datum to which the simulation referred was the presence or not of the groundwater level (GL or not GL in the **Figure 25**).

The results obtained are highlighted in the diagrams of **Figure 25**, which show the trend of the SF versus the cohesion of the altered marls, for two cohesion conditions (15 and 10 kPa) of intact marls. The diagrams show that to verify instability (SF ≤ 1), two conditions are necessary: (i) the presence of a water table under the

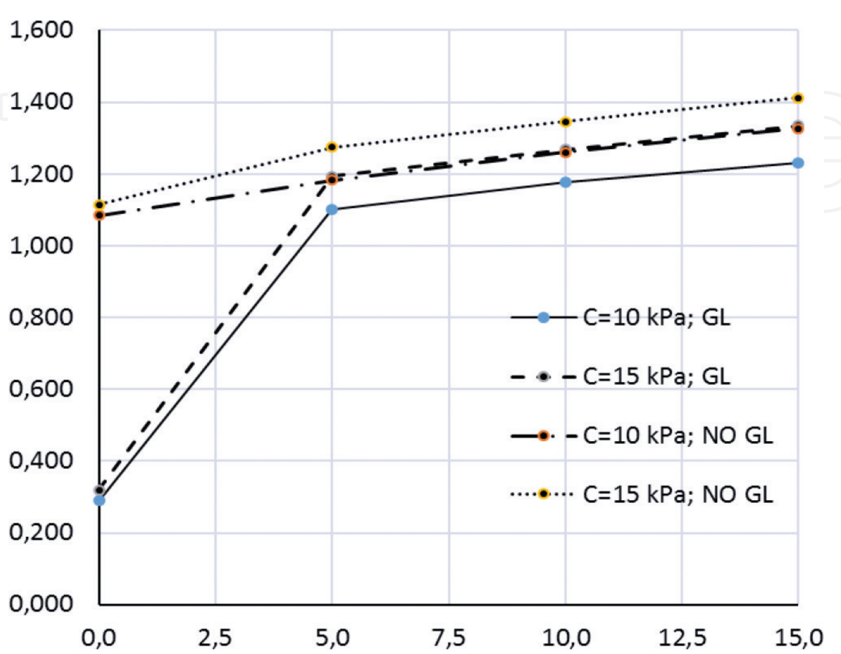

Figure 25.
SF versus altered marlstone's cohesion (kPa) for two conditions of intact marls (C = 10 and 15 kPa) and groundwater level presence (GL) and absent (NO GL).

roadway and (ii) the circulation of water that causes the reduction of cohesion in the altered marls below the value of 5 kPa.

5.2 Road slope instability

The results show that the groundwater presence (GL) and a consequent reduction in cohesion of the altered marl horizon determine a drastic reduction of the safety factor below the unit value, as illustrated in **Figure 24** (displacement vectors) and in the diagrams of **Figure 25**.

6. Conclusions

Some aspects that are not directly investigated characterize the situations examined. The first one concerns the materials constituting a wall system built in the fifteenth and sixteenth centuries, completely integrated into the city center; this wall system is bordered by an area in which an underground car parking is planned and the excavation could create dangerous conditions for the wall system itself.
In the second case, problems arise from the effects of groundwater in the alluvial soil covering a hill, on the flank of which runs a road. Here, in the case of intense meteoric conditions, the groundwater reaches the foot of the slope and determines its instability, by rotational kinematics, in an unexpected way.

In both cases, traditional geotechnical investigations do not solve the problems. Conversely, geophysical surveys integrate the knowledge framework and provide the fundamental elements for the development of back or sensitivity analysis, which can be performed with numerical methods, based on reliable geomechanical models.

Based on the results obtained, it was possible to conclude that:

- In the first case, it should be noted that to carry out the excavation, preliminary retaining structures (cables, micro piles, etc.) are necessary, whose designing must take into account both the effective wall thickness and the extent of the excavation, whether it will concern only the loose material or even the rock below.

- In the second case, it should be noted that drainage and waterproofing of the slope toward the surrounding land will be necessary.

Conflict of interest

The authors of this chapter declare that in its publication, there is no reason, even potential, of conflict of interest.

Author details

Roberto Balia* and Pier Paolo Manca
Dipartimento di Ingegneria Civile, Ambientale e Architettura, Università di Cagliari, Italy

*Address all correspondence to: balia@unica.it

References

[1] Hudson JA. Rock engineering case histories: Key factors, mechanisms and problems. In: Särkkä, Eloranta, editors. Rock Mechanics—A challenge for society. Proceedings of ISRM Regional Symposium EUROC2001; Espoo, Finland; 4-7 June 2001; Rotterdam: Balkema; 2001

[2] Detournay C, Hart R. FLAC and numerical modelling in geomechanics. In: Proceedings of the International FLAC Symposium on Numerical Modelling in Geomechanics, Minneapolis; Rotterdam: Balkema; 1999

[3] Jing L. Mint: A review of techniques, advances and outstanding issues in numerical modelling for rock mechanics and engineering. International Journal of Rock Mechanics and Mining Sciences. 2003;**40**:283-353

[4] Van Westen CJ et al. Mint: Prediction of the occurrence of slope instability phenomena through GIS-based hazard zonation. Geologische Rundschau. 1997;**86**:404-414

[5] Borja RI. Mint: WJA. Continuum deformation and stability analyses of a steep hillside slope under rainfall infiltration. Acta Geotechnica. 2010;**5**:1-14

[6] Dobrin MB, Savit CH. Introduction to Geophysical Prospecting. 4th ed. New York: McGraw-Hill; 1988. ISBN: 0070171963; 007100404

[7] Foti S, Lai CG, Rix GJ, Strobbia C. Surface Wave Methods for Near-Surface Site Characterization. London: CRC Press; 2017

[8] Palmer D. The Generalized Reciprocal Method of Seismic Refraction Interpretation. Tulsa, Oklahoma: Society of Exploration Geophysicists; 1980. ISBN (Print): 978-0-931830-14-3

[9] Peterson JE, Paulsson BN, McEvilly TV. Mint: Applications of algebraic reconstruction techniques to crosshole seismic data. Geophysics. 1985;**50**:1566-1580

[10] White DJ. Mint: Two-dimensional seismic refraction tomography. Geophysical Journal. 1989;**97**:223-245

[11] Ingber L. Mint: Adaptive simulated annealing (ASA): Lessons learned. Control and Cybernetics. 1996;**25**(1):33-54

[12] Montgomery DR. Mint: Road surface drainage, channel initiation, and slope instability. Water Resources Research. 1994;**30**:1925-1932

[13] Fourie AB. Predicting rainfall-induced slope instability. Proceedings of the Institution of Civil Engineers: Geotechnical Engineering. 1996;**119**(4):211-218